Resonant tunneling of carriers in silicon nanocrystals

N. V. Derbenyova, A. A. Konakov, and V. A. Burdov
N.I. Lobachevsky State University of Nizhny Novgorod, Nizhny Novgorod Oblast 603950, Russia

(Received 20 August 2016; accepted 19 September 2016; published online 3 October 2016)

The rates of resonant and nearly resonant tunnel transitions have been calculated within the envelope function approximation for electrons and holes in silicon nanocrystals embedded in a silicon dioxide matrix. It is shown that, if the nanocrystals are close enough, the rates of resonant tunneling reach the values of the order of 10^{12}–$10^{14}\,s^{-1}$, which considerably exceed the rates of radiative recombination and other basic non-radiative processes, such as the Auger recombination and capture on surface defects. The transition rate is found to be very sensitive to inter-crystallite distance, crystallite size, and effective mass of the carriers in the oxide matrix. Electron tunneling turns out to be faster than the hole one, especially, at greater distances between the nanocrystals. Thus, the tunnel migration in a dense ensemble of nanocrystals is mainly electronic. *Published by AIP Publishing*. [http://dx.doi.org/10.1063/1.4963871]

I. INTRODUCTION

Silicon nanocrystals have been the subject of extensive study for the last 20–25 years because of their potential applications in nano-photonics and (recently) photovoltaics. A lot of works were devoted to the investigation of structural, electronic, transport and optical properties of Si crystallites (see, e.g., Refs. 1–6 and references therein for review) as well as to their use in various Si-based devices.[7] However, in experimental samples and device applications, one has to deal not with individual nanocrystals but rather with their ensembles formed in various wide-band matrices, in which nanocrystals "interact" via the transfer of electrons, holes, or excitons. Such a transfer manifests oneself in experiments[8–10] and, as a rule, affects the luminescence.

One of the possible, and the most efficient, mechanisms of a non-radiative energy transfer in the ensembles of nanocrystals is a tunnel migration of elementary excitations. Frequently, the tunnel dynamics precisely determines the system behavior and characteristics.[11,12] For silicon nanocrystals in the SiO_2 matrix, this process turns out to be efficient enough compared to, e.g., radiative interband recombination. The rates of non-resonant phonon-assisted tunnel transitions[13,14] can essentially exceed the rates of electron-hole recombination accompanied by photon emission. The latter rates are less than $10^5\,s^{-1}$ as a rule.[1,15–17] As a consequence, tunnel migration considerably modifies the spectrum of luminescence in an ensemble of silicon nanocrystals. In particular, it was shown earlier[1,18] that tunnel transitions strongly suppress light emission from the smaller nanocrystals in the ensemble. This leads to a remarkable effective redshift of the luminescent peak with respect to its position expected from the size distribution of the nanocrystals.

At the same time, the rates of the non-resonant tunnel migration are less than, or of the same order of magnitude as, the rates of various non-radiative processes occurring in nanocrystals independently of the presence, or absence, of "neighbors". Among all these processes, we can point out three fastest ones: the Auger recombination whose rates can achieve $10^{12}\,s^{-1}$;[19–22] capture on dangling bonds with the rates up to $10^{10}\,s^{-1}$;[23] and relaxation by impact ionization with the rates not greater, as a rule, than $\sim 10^{14}\,s^{-1}$.[24–26] The tunneling of carriers is sensitive to both crystallite sizes and inter-crystallite distance. When the nanocrystals touch one another, the rates of the non-resonant tunneling are high enough: 10^7–$10^{12}\,s^{-1}$ depending on the relationship between the nanocrystal sizes. As the inter-crystallite distance increases up to 1 nm, the rates exponentially drop to 10^2–$10^8\,s^{-1}$.[13,14]

If the sizes of adjacent nanocrystals, in which the tunnel transition takes place, are very close, then the carrier tunneling becomes resonant and can be a very fast (perhaps even fastest) process in the ensemble. Below, within the framework of the envelope function approximation applied to nanocrystals with radii up to 5 nm, we estimate the rates of such resonant transitions and show that their values, indeed, turn out to be high enough when the nanocrystals are in close proximity. Besides, the role of the host matrix is examined. It is shown in particular, that discontinuity of the effective mass at the Si/SiO_2 interface strongly influences the rate of the resonant tunneling.

Frequently, when modelling electron transport through SiO_2 layers containing Si nanocrystals, the tunnel transitions are treated within the framework of the one-dimensional model based on the WKB approach (see, e.g., Refs. 27–30), which is adopted for the three-dimensional objects—quantum dots. Such an approximation is, obviously, too crude and does not allow to describe correctly the effect of the nanocrystal shape on the carrier tunneling. Here, we take into account the sphericity of the nanocrystals and analyze the dependence of the tunneling rate on the nanocrystal radius.

II. THE MODEL

Let us consider two Si nanocrystals with radii R_1 and R_2 closely situated in a wide-band matrix. For definiteness, we set $R_1 < R_2$. The inter-crystallite distance (equal to a minimal distance between the nanocrystals' edges) is denoted as L. We suppose that initially, electron occupies the ground state in the "conduction band" of the smaller nanocrystal, which is called hereafter as "first". Then, this electron

tunnels into the greater ("second") nanocrystal and populates its ground state in the "conduction band". The "valence bands" of both the nanocrystals are supposed to be fully occupied under the transition, as shown in Fig. 1(a). Similarly, the hole tunnel transition occurs at the empty conduction band of both the nanocrystals and one unoccupied valence ground state that was situated in the first nanocrystal before tunneling (see Fig. 1(b)).

In this study, we assume that the sizes of the two adjacent nanocrystals differ very weakly, i.e., $\delta R \equiv R_2 - R_1 \ll R \equiv (R_1 + R_2)/2$, and absolute value of the difference of the ground-state energies $|\varepsilon_1 - \varepsilon_2|$ in the nanocrystals is of the order of, or less than, the level width 2γ equal to $\sim$20 meV.[23,31] This, in fact, means that the tunneling is resonant. It should be noted that in the considered case the tunnel transition occurs with reducing the energy because $\varepsilon_1 > \varepsilon_2$. In the opposite case, the system has to increase its energy by $\Delta\varepsilon = \varepsilon_1 - \varepsilon_2$. This leads to $\exp(\Delta\varepsilon/k_BT)$-fold weakening the transition probability, as has been already pointed out.[32,33]

We shall use a single-particle approximation neglecting the Coulomb effects. Such an approach is justified if size-quantization energies are much greater than the typical Coulomb energies. This condition is satisfied for nanocrystals whose sizes do not exceed several ($\sim$10) nanometers. Such nanocrystals are precisely considered here. Evidently, the suggested scheme of electron or hole tunneling in Fig. 1 seems most preferable from the point of view of a single-particle picture, since the tunneling is not accompanied by the creation or destruction of an exciton in any of the two nanocrystals in this case. Therefore, the total Coulomb energy of the system does not change, and the Coulomb blockade effects do not appear. However, note that the system turns out to be negatively or positively charged.

III. RESULTS AND DISCUSSION

The rate of resonant tunnel transition from the ground state of the first nanocrystal with the wave function ψ_1 to the ground state of the second nanocrystal with the wave function ψ_2 can be formally described by the Fermi's golden rule

$$\tau^{-1} = \frac{2\pi}{\hbar}|\langle\psi_1|U(\mathbf{r}-\mathbf{b})|\psi_2\rangle|^2\rho(\varepsilon_1-\varepsilon_2) \qquad (1)$$

despite the stationary type of the perturbation inducing the transition. Here, the potential energy of the electron in the second nanocrystal is taken as a perturbation. The center of the second nanocrystal is displaced by the vector $\mathbf{b}$ with respect to the coordinate origin situated in the center of the first nanocrystal. Potential energy $U(\mathbf{r}-\mathbf{b})$ provides, in fact, an opportunity of the tunnel transition, since the potential barrier between the nanocrystals has the finite width. The density of states $\rho(x)$ is a broadened δ-function that can be approximated as follows:

$$\rho(x) = \frac{\gamma/\pi}{\gamma^2 + x^2}.$$

Precisely, due to this function, the no-phonon (or no-photon) tunnel transitions may take place in the absence of an exact resonance, when the energies ε_1 and ε_2 are close but do not coincide. In fact, typical width of the function $\rho(x)$ defines a permissible measure of the energy non-conservation under the transition.

For simplicity, we do not take into account the possible lattices' disorientation in the first and second nanocrystals, as well as distinction in the crystal lattices of the oxide matrix and silicon (moreover, the matrix can be amorphous and not at all have any crystal structure). This, in particular, implies an identity of the Bloch functions inside and outside both the nanocrystals from the point of view of the envelope function approximation employed here. The outer region will be modelled by the potential barrier with the height equal to the band offset, and some value of the effective mass different from the one in the nanocrystals. Made approximations, of course, have no rigorous substantiation but seem quite sufficient for estimating the typical tunneling rates.

Based on the above assumptions, we can use the s-type ground state envelope functions in Eq. (1)

$$\psi(r<R) = \frac{\sin(kr)/r}{\sqrt{2\pi R\left(1+\frac{1}{\kappa R}\cdot\frac{\alpha\kappa R + k^2R^2}{\alpha^2+k^2R^2}\right)}},$$
$$\psi(r>R) = \frac{\sin(kR)\exp(-\kappa(r-R))/r}{\sqrt{2\pi R\left(1+\frac{1}{\kappa R}\cdot\frac{\alpha\kappa R + k^2R^2}{\alpha^2+k^2R^2}\right)}} \qquad (2)$$

instead of the total wave functions. Here, energy ε is counted from the top of the barrier, and the parameters α, k, and κ are defined as $\alpha = (1+\kappa R)m_{in}/m_{out} - 1$, $k = \sqrt{2m_{in}(\varepsilon+U)}/\hbar$, and $\kappa = \sqrt{-2m_{out}\varepsilon}/\hbar$, respectively, where U stands for the band offset and m_{in} and m_{out} are isotropic effective masses of the carrier inside and outside the nanocrystals, respectively. Electron isotropic effective mass inside the nanocrystals is

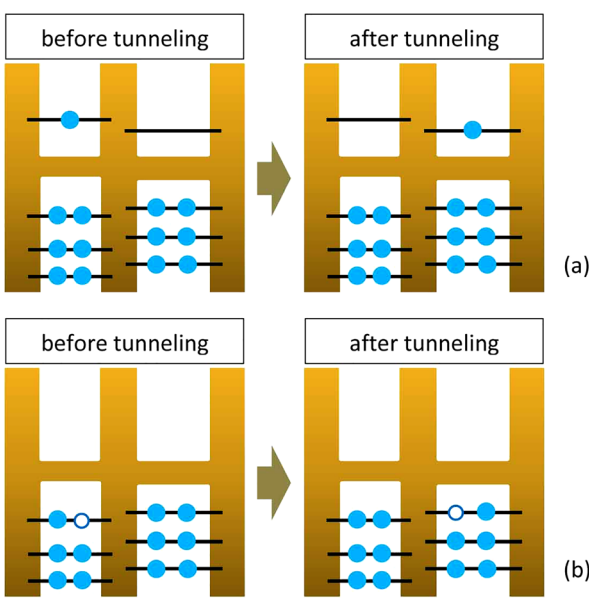

FIG. 1. Schematic representation of the electron (a) and hole (b) tunnel transitions from the smaller ("first") nanocrystal to the greater ("second") one.

defined by the following relation: $1/m_{\text{in}}^{(e)} = (m_l^{-1} + 2m_t^{-1})/3$,[34,35] where m_l and m_t are longitudinal and transverse effective masses equal to 0.92 and 0.19, respectively, of the free electron mass m_0. Thus, $m_{\text{in}}^{(e)} = 0.26m_0$. For the hole ground state inside the nanocrystal, one can set $m_{\text{in}}^{(h)} = m_0/A$,[34,35] where number $A = 4.22$ is a standard parameter of the kp-matrix in the Γ'_{25} valence band,[36] so that $m_{\text{in}}^{(h)} = 0.24m_0$. Outside the nanocrystals, in the forbidden band of SiO_2 matrix, the effective masses of the electrons and holes, presumably, are not known exactly. Frequently, in various experiments on electron transport through SiO_2 layers (see, e.g., Refs. 37 and 38), as well as in computational simulations,[29,30] the electron and hole effective masses are determined as $m_{\text{out}}^{(e)} \sim 0.4m_0$ and $m_{\text{out}}^{(h)} \sim 0.3m_0$. Other authors assume the electron effective mass $m_{\text{out}}^{(e)}$ equal to the free electron mass m_0,[5,17,39] while $m_{\text{out}}^{(h)}$ is assumed to be five[17,40] or, even, ten[5] times greater. Here, we follow Refs. 17, 39, and 40 and set $m_{\text{out}}^{(e)} = m_0$, $m_{\text{out}}^{(h)} = 5m_0$, and $m_{\text{in}}^{(e)} = m_{\text{in}}^{(h)} = 0.25m_0$ for simplicity. Possible changes in the obtained results caused by another choice of m_{out} will be discussed in Section IV (Concluding remarks).

The ground state energy can be found from the equation

$$kR\cot(kR) = -\alpha. \tag{3}$$

The barrier height U equals U_e or U_h for the electron or hole, respectively. The values of the band offsets for electrons and holes at Si/SiO_2 interface can be taken as $U_e = 3.2$ eV and $U_h = 4.5$ eV, respectively.[41]

Now, we calculate the matrix element

$$\begin{aligned}\langle\psi_1|U(\mathbf{r}-\mathbf{b})|\psi_2\rangle &= -U\iiint\limits_{|\mathbf{r}-\mathbf{b}|<R}\psi(r)\psi(|\mathbf{r}-\mathbf{b}|)d\mathbf{r}\\ &= -U\iiint\limits_{r<R}\psi(r)\psi(|\mathbf{r}-\mathbf{b}|)d\mathbf{r}\end{aligned} \tag{4}$$

defining the transition rate [Eq. (1)]. When calculating, we set $R_1 = R_2 = R$ and $\varepsilon_1 = \varepsilon_2 = \varepsilon$. Correspondingly, the parameters α, k, and κ do not depend on the nanocrystal "number". Substitution of Eq. (2) into Eq. (4) yields

$$\begin{aligned}\langle\psi_1|U(\mathbf{r}-\mathbf{b})|\psi_2\rangle = &-\frac{Ue^{\kappa R}\sin(kR)}{R+\frac{1}{\kappa}\cdot\frac{\alpha\kappa R+k^2R^2}{\alpha^2+k^2R^2}}\int_0^R r\sin(kr)dr\\ &\times\int_0^\pi d\theta\sin\theta\frac{e^{-\kappa\sqrt{b^2+r^2-2br\cos\theta}}}{\sqrt{b^2+r^2-2br\cos\theta}},\end{aligned}$$

where spherical coordinates (angle θ is counted from the vector $\mathbf{b}$) were used. After integrating, one obtains in the limiting case $\kappa R \gg 1$ or, similarly, $\kappa \gg k$ (i.e., $\varepsilon + U \ll U$)

$$\langle\psi_1|U(\mathbf{r}-\mathbf{b})|\psi_2\rangle = -\frac{R(\varepsilon+U)}{mb}\frac{(\kappa R+\alpha)\exp(-\kappa L)}{\kappa R(\alpha^2+\alpha+k^2R^2)+k^2R^2},$$

where $m = m_{\text{out}}/m_{\text{in}}$, and $b = L + R_1 + R_2 = L + 2R$ is the distance between the nanocrystals' centers.

As a result, the rate of the tunnel transition has the form

$$\begin{aligned}\tau^{-1} = &\frac{\exp(-2\kappa L)}{2\hbar(1+L/2R)^2}\left(\frac{\varepsilon+U}{m}\right)^2\\ &\times\left(\frac{\kappa R+\alpha}{\kappa R(\alpha^2+\alpha+k^2R^2)+k^2R^2}\right)^2\frac{\gamma}{\gamma^2+(\varepsilon_1-\varepsilon_2)^2},\end{aligned} \tag{5}$$

where $\varepsilon = \varepsilon(R)$, while $\varepsilon_{1,2} = \varepsilon(R_{1,2})$. According to this expression, the rate (i) has a resonant profile as function of the energy difference $\varepsilon_1 - \varepsilon_2$ and (ii) nearly exponentially drops with increasing the potential barrier width L. At $\gamma = 10$ meV, $\varepsilon_1 = \varepsilon_2$, and $L = 0$, estimating the rate yields the values ranging within 10^8–$10^{14}\,s^{-1}$ for nanocrystal radii from 1 to 5 nm, as shown in Fig. 2.

As seen from the figure, a very fast decrease of the rate takes place as L increases. In particular, the rate of the electron transition at $L = 1$ nm becomes eight orders of magnitude less than at $L = 0$. At the same time, the hole tunneling rate decays still faster. Its decrement is more than two times greater compared to that of the electron rate. Correspondingly, the hole transition rate reduces its value by eight orders already at $L = 0.4$ nm. Such a behavior is naturally explained by the greater values of the valence band offset U_h and, mainly, of the hole effective mass $m_{\text{out}}^{(h)}$.

It is also seen that the transition rates, for both the electrons and holes, strongly depend on the nanocrystal size. Decrease of the rates in a resonant case, when the nanocrystal sizes exactly coincide, is about four orders of magnitude, as the nanocrystal radius increases from 1 to 5 nm. This dependence is not exponential but rather has a power-type law: $\sim R^{-6}$. It comes from the dependence $\varepsilon(R)$ and the normalization condition of the envelope functions, which define two squared factors (second and third, respectively) in the right side of Eq. (5).

It is worth noting that the electron tunneling rate is always (especially at greater L) substantially greater than the

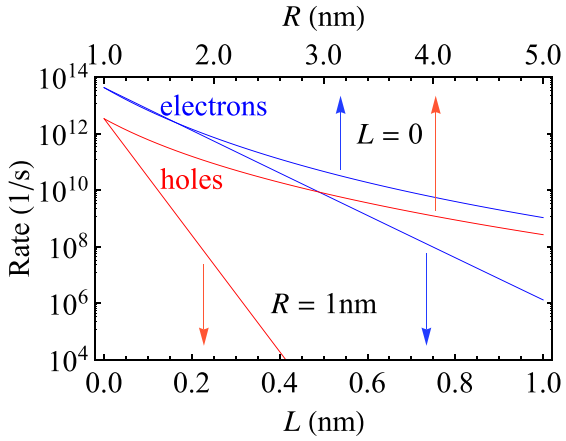

FIG. 2. Resonant ($\delta R = 0$) electron and hole tunneling rates as functions of inter-crystallite distance L (lower horizontal axis) at $R = 1$ nm and crystallite radius R (upper horizontal axis) at $L = 0$.

hole one. This means that the tunnel migration in a dense ensemble of Si nanocrystals in the SiO_2 matrix will occur mainly through the electron "channel", while the hole tunneling turns out to be considerably slower process. Nevertheless, at distances L less than ~0.2 nm, the hole tunnel migration remains comparable in rate with other non-radiative processes, such as the Auger recombination and capture on dangling bonds.

It is also important to emphasize that the rates of resonant tunneling are at least two orders of magnitude greater than those of non-resonant phonon-assisted tunnel transitions. As has been already pointed out in Introduction, the maximum rate values for the non-resonant tunneling do not exceed $10^{12}\,s^{-1}$ according to the estimations done earlier.[13,14] Moreover, these estimations have been carried out in supposition that the electron and hole effective masses outside the nanocrystals equal their values inside. Evidently, this yields slightly overestimated values of the transition rates.

Indeed, this conclusion can be indirectly corroborated by the calculations performed for the resonant case. In Fig. 3, we have plotted the resonant transition rates both for the electrons and holes versus dimensionless mass parameter m for touching nanocrystals with radii $R_1 = R_2 = R = 2$ nm. It is convenient to assume the effective masses m_{in} and m_{out} to be fixed and varied, respectively, so that m varies from 1 to 40. As Fig. 3 shows, the rates substantially decrease as m_{out} increases with respect to m_{in} for both the electrons and holes. In particular, at the accepted here values of m_{in} and m_{out} corresponding to $m = 4$ for electrons and $m = 20$ for holes (as indicated by the arrows in the figure), the electron tunneling decelerates almost quintuply, while the hole transitions become more than ten times slower compared to the case where $m_{out} = m_{in}$, i.e., $m = 1$. The dependence on the effective mass turns out to be approximately $1/m^4$ at $L = 0$ and $m \gg 1$, as followed from Eq. (5). If the inter-crystallite distance is finite, the decay becomes faster and gains exponential-like character: $m^{-4}\exp(-\lambda\sqrt{m})$ with λ being some constant proportional to L.

Obviously, it is natural to suppose that the non-resonant tunneling rates similarly decrease if the effective mass discontinuity is taken into account. Therefore, it is possible to expect even greater (than two orders of magnitude)

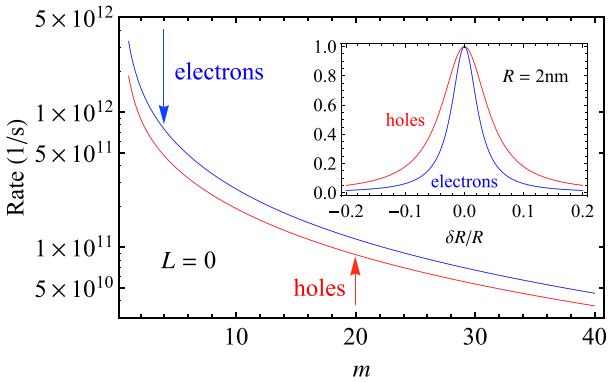

FIG. 3. Resonant tunneling rate as function of the effective mass ratio m at $L = 0$ and $R = 2$ nm. Arrows indicate τ^{-1} on the curves for used in the paper values of the electron and hole effective masses, which correspond to $m = 4$ for electrons and $m = 20$ for holes. Inset: resonance profile as function of the relative radius discrepancy.

difference in the rates of resonant and non-resonant tunnel migration. Typical resonance width recalculated from the energy scale to the radius one is about 0.1 nm, as shown in the inset to Fig. 3, where the tunneling rate normalized to its maximum (resonant) value

$$f = \frac{\tau^{-1}(\varepsilon_1, \varepsilon_2)}{\tau^{-1}(\varepsilon_1 = \varepsilon_2)} = \frac{\gamma^2}{\gamma^2 + (\varepsilon_1 - \varepsilon_2)^2}$$

has been depicted as function of the relative radius discrepancy. If the latter becomes greater than ~0.1, tunneling turns into the non-resonant and requires phonon assistance to be occurred.

IV. CONCLUDING REMARKS

In conclusion, we would like to touch upon briefly the issue of the chosen values m_{out} for electrons and holes in the SiO_2-matrix, as was noticed in Section III. According to the obtained results presented, in particular, in Fig. 3, the choice of these values crucially influences the rates of the tunnel transitions. It is seen that the rates vary within sufficiently wide range (~two orders of magnitude or, even, more at nonzero L) for different values of dimensionless mass m. Consequently, the choice of m can be, indeed, of great importance for calculations. As has been already mentioned above, the values m_{out} we have chosen may not be considered as fully conventional. Instead, the values from 0.3 to 0.5 have been suggested for m_{out}/m_0,[28–30,37,38] which correspond to $1.2 \le m \le 2$. It is important that $m_{out}^{(e)}$ and $m_{out}^{(h)}$ were reported to be very close: e.g., 0.4 and 0.33 of m_0, respectively, in Ref. 38. As a result, the difference in the tunneling rates for the electrons and holes is not so strong as was found at chosen here values of $m_{out}^{(e)}$ and $m_{out}^{(h)}$. Nevertheless, as before, the electron tunneling remains faster than the hole one due to the smaller barrier height for electrons. It is necessary to note also that the decrease of m leads to the increase of the transition rate. Therefore, the electron and hole transition rates will be even greater in this case than the rates obtained in the present work. Thus, the main conclusion of this paper that the resonant tunnel migration of electrons and holes turns out to be one of the fastest and efficient non-radiative processes in the closely packed ensembles of Si nanocrystals remains valid.

Note finally that, here, we do not consider the exciton tunneling that, in principle, can also take place in the ensembles of (Si) nanocrystals. Obviously, the joint tunnel transitions of electron and hole require much more time to be occurred than the explored here individual transitions of the carriers, i.e., the exciton transition will be a much slower process than that of the electron or hole. We have considered only the fastest processes because of their higher significance for various experimental situations. Therefore, the exciton tunneling remains beyond the frames of our study.

ACKNOWLEDGMENTS

The authors sincerely thank professor I. N. Yassievich for her interest to this work and fruitful discussions. The work was supported by the Ministry of Education and Science of Russian Federation (project No 2696).

[1]V. A. Belyakov, V. A. Burdov, R. Lockwood, and A. Meldrum, Adv. Opt. Technol. **2008**, 279502 (2008).
[2]I. Balberg, J. Appl. Phys. **110**, 061301 (2011).
[3]L. Khriachtchev, S. Ossicini, F. Iacona, and F. Gourbilleau, Int. J. Photoenergy **2012**, 872576 (2008).
[4]S. K. Ray, S. Maikap, W. Banerjee, and S. Das, J. Phys. D: Appl. Phys. **46**, 153001 (2013).
[5]O. B. Gusev, A. N. Poddubny, A. A. Prokofiev, and I. N. Yassievich, Semiconductors **47**, 183 (2013).
[6]E. G. Barbagiovanni, D. J. Lockwood, P. J. Simpson, and L. V. Goncharova, Appl. Phys. Rev. **1**, 011302 (2014).
[7]F. Priolo, T. Gregorkiewicz, M. Galli, and T. F. Krauss, Nat. Nanotechnol. **9**, 19 (2014).
[8]J. Heitmann, F. Muller, L. Yi, M. Zacharias, D. Kovalev, and F. Eichhorn, Phys. Rev. B **69**, 195309 (2004).
[9]Z. Lin, H. Li, A. Franceschetti, and M. T. Lusk, ACS Nano **6**, 4029 (2012).
[10]R. Limpens, A. Lesage, P. Stallinga, A. N. Poddubny, M. Fujii, and T. Gregorkiewicz, J. Phys. Chem. C **119**, 19565 (2015).
[11]A. Anopchenko, A. Marconi, M. Wang, G. Pucker, P. Bellutti, and L. Pavesi, Appl. Phys. Lett. **99**, 181108 (2011).
[12]A. Shabaev, A. L. Efros, and A. L. Efros, Nano Lett. **13**, 5454 (2013).
[13]V. A. Belyakov, K. V. Sydorenko, A. A. Konakov, N. V. Kurova, and V. A. Burdov, J. Phys.: Conf. Ser. **245**, 012039 (2010).
[14]V. A. Belyakov and V. A. Burdov, Quantum Matter **4**, 85 (2015).
[15]M. S. Hybertsen, Phys. Rev. Lett. **72**, 1514 (1994).
[16]C. Delerue, G. Allan, and M. Lannoo, Phys. Rev. B **64**, 193402 (2001).
[17]A. S. Moskalenko, J. Berakdar, A. A. Prokofiev, and I. N. Yassievich, Phys. Rev. B **76**, 085427 (2007).
[18]V. A. Belyakov, K. V. Sidorenko, A. A. Konakov, A. V. Ershov, I. A. Chugrov, D. A. Grachev, D. A. Pavlov, A. I. Bobrov, and V. A. Burdov, J. Lumin. **155**, 1 (2014).
[19]N. V. Kurova and V. A. Burdov, Semiconductors **44**, 1414 (2010).
[20]C. I. Mihalcescu, J. C. Vial, A. Bsiesy, F. Muller, R. Romestain, E. Martin, C. Delerue, M. Lannoo, and G. Allan, Phys. Rev. B **51**, 17605 (1995).
[21]C. Sevik and C. Bulutay, Phys. Rev. B **77**, 125414 (2008).
[22]M. Mahdouani, R. Bourguiga, S. Jaziri, S. Gardelis, and A. G. Nassiopoulou, Physica E **42**, 57 (2009).
[23]M. Lannoo, C. Delerue, and G. Allan, J. Lumin. **70**, 170 (1996).
[24]G. Allan and C. Delerue, Phys. Rev. B **79**, 195324 (2009).
[25]C. Delerue, G. Allan, J. J. H. Pijpers, and M. Bonn, Phys. Rev. B **81**, 125306 (2010).
[26]M. Govoni, I. Marri, and S. Ossicini, Nat. Photonics **6**, 672 (2012).
[27]X. D. Pi, O. H. Y. Zalloum, A. P. Knights, P. Mascher, and P. J. Simpson, J. Phys.: Condens. Matter **18**, 9943 (2006).
[28]J. Carreras, C. Bonafos, J. Montserrat, C. Dominguez, J. Arbiol, and B. Garrido, Nanotechnology **19**, 205201 (2008).
[29]J. Carreras, O. Jambois, S. Lombardo, and B. Garrido, Nanotechnology **20**, 155201 (2009).
[30]N. Garcia-Castello, S. Illera, D. Prades, S. Ossicini, A. Cirera, and R. Guerra, Nanoscale **7**, 12564 (2015).
[31]G. Allan and C. Delerue, Phys. Rev. B **75**, 195311 (2007).
[32]H. E. Roman and L. Pavesi, J. Phys.: Condens. Matter **8**, 5161 (1996).
[33]L. Pavesi, J. Appl. Phys. **80**, 216 (1996).
[34]V. A. Burdov, Semiconductors **36**, 1154 (2002).
[35]V. A. Burdov, JETP **94**, 411 (2002).
[36]*Landolt-Börnstein Tables*, edited by O. Madelung, M. Schulz, and H. Weiss (Springer, Berlin, Heidelberg, 1987), v. 22a.
[37]M. I. Vexler, S. E. Tyaginov, and A. F. Shulekin, J. Phys.: Condens. Matter **17**, 8057 (2005).
[38]R. Ludeke, E. Cartier, and A. Schenk, Appl. Phys. Lett. **75**, 1407 (1999).
[39]J. M. Ferreira and C. R. Proetto, Phys. Rev. B **60**, 10672 (1999).
[40]J. R. Chelikowsky and M. Schlüter, Phys. Rev. B **15**, 4020 (1977).
[41]R. M. Wallace and G. D. Wilk, Semicond. Int. **8**, 227 (2001).